Ordered ground state wurtzite alloys from zinc-blende parent compounds

H. J. Xiang and Su-Huai Wei

National Renewable Energy Laboratory, Golden, Colorado 80401, USA

Shiyou Chen and X. G. Gong

Surface Science Laboratory and Department of Physics, Fudan University, Shanghai 200433, China

The ground state structures of the $A_xB_{1-x}C$ wurtzite (WZ) alloys with $x=0.25$, 0.5, and 0.75 are revealed by a ground state search using the valence-force field model and density-functional theory total-energy calculations. It is shown that the ground state WZ alloy always has a lower strain energy and formation enthalpy than the corresponding zinc-blende (ZB) alloy. Therefore, we propose that the WZ phase can be stabilized through alloying. This idea is supported by the fact that the WZ $AlP_{0.5}Sb_{0.5}$, $AlP_{0.75}Sb_{0.25}$, $ZnS_{0.5}Te_{0.5}$, and $ZnS_{0.75}Te_{0.25}$ alloys in the lowest-energy structures are more stable than the corresponding ZB alloys. In this example, the alloy adopts a structure distinct from both parent phases.

PACS number(s): 61.50.Ah, 61.66.Dk, 64.70.kg, 71.15.Nc

III-V and II-VI semiconductors usually crystallize into one of two forms: hexagonal wurtzite (WZ) and cubic zinc-blende (ZB) structures, which have the same local tetrahedral environment. Despite the structural similarity, there are some significant differences in the electronic and optical properties.[1,2] Compared to the hexagonal structure, the cubic phase has a more isotropic property, higher carrier mobility, lower phonon scattering, and often better doping efficiency. In contrast, the WZ phase has a larger band gap (usually direct), a spontaneous electric polarization, and a lower propagating speed of dislocations and thus an improved lifetime of the laser diodes.[3] For certain device applications, one phase is preferred over the other. To have a controllable way to synthesize the desired phase, it is important to understand the mechanism for stabilizing a certain structure.

In general, the WZ structure is preferred over the ZB structure when the ionicity of a compound is high.[4] This is because the ideal WZ structure has a larger Coulomb interaction energy with a larger Madelung constant, whereas the ZB structure leads to a better covalent-bond formation.[5–8] To change the stability, one often grows materials into different forms. For example, many ZB compounds can adopt the hexagonal WZ structure when forming nanowires (NWs).[9–11] Empirical calculations suggested that the stability of the WZ NW is due to the fact that the WZ NW has less surface atoms than the ZB NW with a similar diameter.[12,13] Theoretical calculations also showed that stability of WZ compounds such as GaN can be changed when carriers are introduced through doping.[14,15] Moreover, metastable phases can be synthesized by employing nonequilibrium growth techniques. For example, metastable ZB GaN can be grown on cubic substrates.[16]

In this paper, we show that the ground state (GS) WZ alloy (WZA) always has a lower strain energy than the corresponding ZB alloy (ZBA). Therefore, if strain energy is dominant in alloy formation, stable GS ternary WZAs can form even though the binary constituents are more stable in the ZB phase. This provides an opportunity to form desired WZAs through alloying. Our first-principles calculations confirm this idea, showing that WZ $AlP_{0.5}Sb_{0.5}$, $AlP_{0.75}Sb_{0.25}$, $ZnS_{0.5}Te_{0.5}$, and $ZnS_{0.75}Te_{0.25}$ have lower total energies than

the ZB counterparts. In this work, we consider the ground state at 0 K without including the negligible configuration entropy.

The GS structures of ZBAs have been extensively studied.[17–21] For instance, it was shown that the GS ZB $A_{0.5}B_{0.5}C$ alloy (without loss of generality, B ion is assumed to have a larger radius than A ion, and C could be anion or cation) adopts the tetragonal chalcopyrite structure (space group $I\bar{4}2d$, No. 122).[17] And the Q8 or Q16 are the possible lowest-energy structures of ZB $A_{0.25}B_{0.75}C$ and $A_{0.75}B_{0.25}C$ alloys.[21] However, the knowledge of the GS structures of WZAs remains incomplete. Our previous work[22] showed that the GS structure of the $A_{0.5}B_{0.5}C$ WZA is of the β-NaFeO$_2$ type with the space group $Pna2_1$ (No. 33) as shown in Fig. 1(a). Here, in this work, we identify that the GS structures of $A_{0.25}B_{0.75}C$ and $A_{0.75}B_{0.25}C$ WZAs have the structures shown in Fig. 1(c) or 1(d) with the space group $P2_1$ (No. 4).

The formation enthalpy of isovalent semiconductor alloys $A_xB_{1-x}C$ is defined as

$$\Delta H_f = E(x) - [xE_{AC} + (1-x)E_{BC}], \qquad (1)$$

where E_{AC}, E_{BC}, and $E(x)$ are the total energies of bulk AC and BC, and the $A_xB_{1-x}C$ alloy with the same crystal structure (WZ or ZB). It is well known that for lattice-mismatched isovalent semiconductor alloys, the major contribution to the formation enthalpy is the strain energy. The strain energy (E_s) could be described well by the valence-force field (VFF) model,[23–25] which considers the deviation of the nearest-neighbor bond lengths and bond angles from the ideal bulk values. Here, we consider all possible super-cells with up to 32 atoms per unit cell. For each supercell, we consider all possible configurations of alloys with $x=0.25$ and 0.75. The VFF model is used to relax the structure and predict the energy of the configuration. We considered $Ga_xIn_{1-x}N$, AlP_xSb_{1-x}, ZnS_xTe_{1-x}, and GaP_xAs_{1-x}. They have various degrees of lattice mismatch: 10.1%, 11.5%, 11.8%, and 3.7%. Our calculations reveal the Lazarevicite structure (space group $Pmn2_1$, No. 31) shown in Fig. 1(b) has the lowest strain energy for $A_{0.25}B_{0.75}C$ for all four different sets
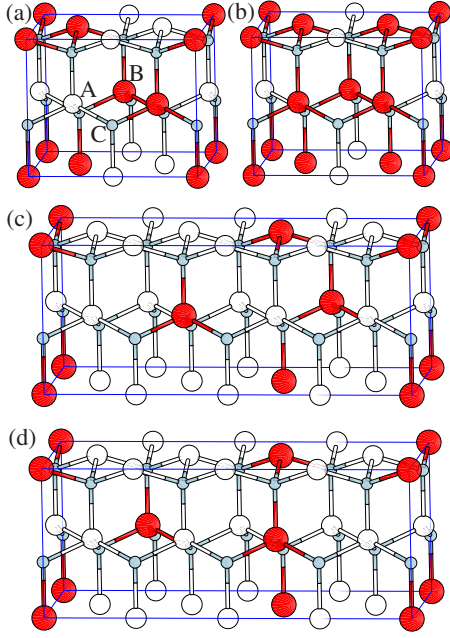
FIG. 1. (Color online) (a) The GS $Pna2_1$ structure of the WZ $A_{0.5}B_{0.5}C$ alloy. (b) The $Pmn2_1$ structure, which is the lowest strain energy structure of the WZ $A_{0.25}B_{0.75}C$ alloy. (c) The lowest strain energy structure ($P2_1$−I) of the WZ $A_{0.75}B_{0.25}C$ alloy. (d) The low strain energy structure ($P2_1$−II) of the WZ $A_{0.75}B_{0.25}C$ alloy.

of VFF parameters.[25,26] The $Pmn2_1$ $A_{0.25}B_{0.75}C$ structure has the same supercell as the $Pna2_1$ $A_{0.5}B_{0.5}C$ structure. One can get the $Pmn2_1$ $A_{0.25}B_{0.75}C$ structure by replacing one half of the A atoms in the $Pna2_1$ $A_{0.5}B_{0.5}C$ structure with B atoms so that each C atom has one neighbor A atom and three neighbor B atoms. The $Pmn2_1$ WZ $A_{0.25}B_{0.75}C$ structure is similar to the famatinite ZB $A_{0.25}B_{0.75}C$ structure[20] in that they both have similar local environment for C atoms.

For the WZ $A_{0.75}B_{0.25}C$ alloy, we identify two low strain energy structures with the $P2_1$ space group (No. 4) [$P2_1$−I: Fig. 1(c), and $P2_1$−II: Fig. 1(d)]. In contrast to the $Pmn2_1$ $A_{0.75}B_{0.25}C$ structure, there are some C atoms which have four A neighbor atoms in both structures. In this sense, the $P2_1$−I and $P2_1$−II WZ $A_{0.75}B_{0.25}C$ structures are similar to the Q8 and Q16 ZB $A_{0.75}B_{0.25}C$ structures.[17,19] As shown in Table I, the $P2_1$−I structure has the lowest strain energy. However, the strain energy difference between the $P2_1$−II and $P2_1$−I structures is very small, less than 0.3 meV/atom.

To see if the GS structures predicted by VFF strain energy calculations are consistent to the density-functional theory (DFT) total-energy calculations, we performed DFT calculations[27–30] on the WZ $A_{0.25}B_{0.75}C$ and $A_{0.75}B_{0.25}C$ alloys with the $Pmn2_1$, $P2_1$−I, and $P2_1$−II structures. Our results are shown in Table I. We can see that the $Pmn2_1$ structure is not the GS of the WZ $A_{0.25}B_{0.75}C$ alloy because the $P2_1$ structures have a slightly lower total energy, even though the $Pmn2_1$ structure has a lower strain energy. This can be explained in terms of the Coulomb interaction. For the $A_xB_{1-x}C$ alloy, the charge of A ions is different from that of B ions due to the different electronegativity. In this case, the Coulomb interaction is found to stablize the $P2_1$ structures over the $Pmn2_1$ structure because the $P2_1$ structures

TABLE I. VFF-calculated strain energy (in meV/atom) of WZ $Ga_xIn_{1-x}N$, AlP_xSb_{1-x}, ZnS_xTe_{1-x}, and GaP_xAs_{1-x} alloys for the $Pmn2_1$, $P2_1$−I, and $P2_1$−II structures at $x=0.25$ and 0.75. The numbers in parenthesis are the DFT-calculated formation enthalpies.

Structures	$Pmn2_1$	$P2_1$−I	$P2_1$−II
$Ga_{0.25}In_{0.75}N$	12.54[a](13.13)	14.13(12.38[b])	14.17(12.50)
$Ga_{0.75}In_{0.25}N$	20.16(16.91)	19.01[a](13.25[b])	19.28(13.47)
$AlP_{0.25}Sb_{0.75}$	19.43[a](18.88)	21.02(18.19[b])	21.20(18.37)
$AlP_{0.75}Sb_{0.25}$	24.41(27.09)	23.46[a](23.35)	23.69(23.32[b])
$ZnS_{0.25}Te_{0.75}$	13.19[a](21.36)	14.19(20.76[b])	14.35(21.05)
$ZnS_{0.75}Te_{0.25}$	15.14(29.36)	14.73[a](26.96)	14.81(26.86[b])
$GaP_{0.25}As_{0.75}$	2.32[a](2.26)	2.42(1.99)	2.44(1.96[b])
$GaP_{0.75}As_{0.25}$	2.57(2.48)	2.55[a](2.09[b])	2.58(2.12)

[a]GS structures obtained from the VFF calculations.
[b]GS structures obtained from the DFT calculations.

has larger charge fluctuation.[31] Similar situation also occurs in ZBAs.[21]

After knowing the GS structures, we now compare the strain energy of the ZBA and WZA using the VFF model. For the ground state ZBAs with $x=0.5$, we use the chalcopyrite structure. In order to identify the ground state ZBAs with $x=0.25$, and 0.75, we choose three possible candidates, namely, famatinite, Q8, and Q16, proposed in previous ground state searches.[20,21] Table II shows that the results for ZB $Ga_{0.25}In_{0.75}N$ and $Ga_{0.75}In_{0.25}N$ are in agreement with the previous study.[21] As can be seen from Table III, the GS WZAs always have a lower strain energy than the GS ZBAs for all considered systems ($Ga_xIn_{1-x}N$, AlP_xSb_{1-x}, ZnS_xTe_{1-x}, and GaP_xAs_{1-x} with $x=0.25$, 0.5, and 0.75). The difference in the formation enthalpy mainly depends on the size of the lattice mismatch of alloy: for the first three $A_xB_{1-x}C$ alloys with large lattice mismatch ($\Delta a > 10\%$), the strain energy difference dE_s at $x=0.5$ is around 5 meV/atom whereas, the difference dE_s for $GaP_{0.5}As_{0.5}$ ($\Delta a < 4\%$) is only 0.7 meV/atom.

Our above VFF calculations show that the WZ structure

TABLE II. VFF-calculated strain energy (in meV/atom) of ZB $Ga_xIn_{1-x}N$, AlP_xSb_{1-x}, ZnS_xTe_{1-x}, and GaP_xAs_{1-x} alloys for the famatinite, Q8, and Q16 structures at $x=0.25$ and 0.75. The numbers in parenthesis are the DFT-calculated formation enthalpies.

Structures	Famatinite	Q8	Q16
$Ga_{0.25}In_{0.75}N$	16.56[a](18.65)	16.83(17.79[b])	17.46(18.76)
$Ga_{0.75}In_{0.25}N$	27.66(26.29)	23.93(20.51[b])	23.78[a](20.66)
$AlP_{0.25}Sb_{0.75}$	25.98(27.43)	25.62[a](22.87[b])	26.13(23.18)
$AlP_{0.75}Sb_{0.25}$	32.30(38.51)	28.98[a](29.56)	28.99(29.46[b])
$ZnS_{0.25}Te_{0.75}$	17.94(28.40)	17.61[a](24.65[b])	18.02(24.85)
$ZnS_{0.75}Te_{0.25}$	20.36(38.61)	18.40[a](31.99[b])	18.57(32.14)
$GaP_{0.25}As_{0.75}$	3.08(3.51)	2.94[a](2.76)	2.97(2.74[b])
$GaP_{0.75}As_{0.25}$	3.40(3.82)	3.129[a](2.94[b])	3.135(2.95)

[a]GS structures obtained from the VFF calculations.
[b]GS structures obtained from the DFT calculations.

TABLE III. Differences in the VFF strain energy (dE_s), DFT formation enthalpy ($d\Delta H_f$), DFT bond energy (dE_b), and DFT total energy (dE_{tot}) between the GS WZAs and ZBAs. Energy is in meV/atom.

	dE_s	$d\Delta H_f$	dE_b	dE_{tot}
$Ga_{0.25}In_{0.75}N$	−4.03	−5.41	−9.53	−14.94
$Ga_{0.5}In_{0.5}N$	−4.61	−5.79	−8.21	−14.00
$Ga_{0.75}In_{0.25}N$	−4.77	−7.25	−6.91	−14.16
$AlP_{0.25}Sb_{0.75}$	−6.18	−4.68	5.76	1.08
$AlP_{0.5}Sb_{0.5}$	−7.35	−6.50	5.01	−1.49
$AlP_{0.75}Sb_{0.25}$	−5.52	−6.14	4.27	−1.87
$ZnS_{0.25}Te_{0.75}$	−4.42	−3.89	5.33	1.44
$ZnS_{0.5}Te_{0.5}$	−5.18	−5.43	4.62	−0.81
$ZnS_{0.75}Te_{0.25}$	−3.67	−5.12	3.90	−1.22
$GaP_{0.25}As_{0.75}$	−0.62	−0.78	10.75	9.97
$GaP_{0.5}As_{0.5}$	−0.74	−1.05	10.12	9.07
$GaP_{0.75}As_{0.25}$	−0.39	−0.85	9.48	8.63

has a better ability to accommodate the strain in a lattice mismatched alloy than the ZB structure. This is due to the fact that the WZ structure has a larger degree of freedom to release the strain. First, for the binary compound, the four-atoms unit-cell WZ structure has three free parameters (a, c, u). In contrast, the two-atoms unit-cell ZB structure only has one free parameter (a). Second, the WZA is also more flexible than the ZBA. As an example, we compare the 16-atoms WZ $Pna2_1$ and 8-atoms ZB chalcopyrite structures. In both structures, each C atom bonds with two A and two B atoms. In the ZB $A_{0.5}B_{0.5}C$ chalcopyrite structure, there are three free parameters. However, there are fifteen free parameters in the WZ $Pna2_1$ structure. The larger number of degree of freedom in the WZ $Pna2_1$ structure leads to an enhanced flexibility in strain relaxation.

For a better understanding of the strain relaxation in WZAs, we can also decompose the total strain energy into the contributions from each atom.[32] In this way, we can tell which kind of atoms are mainly responsible for the different behavior between the WZ and ZB alloys. This analysis shows that the main difference comes from the B ions with a large size. For example, the total contributions to the strain energy in the chalcopyrite ($Pna2_1$) $AlP_{0.5}Sb_{0.5}$ alloy (here $A=P$, $B=Sb$, and $C=Al$) from Al, P, and Sb are 23.7 (22.6), 2.2 (1.4), and 7.4 (1.9) meV/atom, respectively. We can see that the strain energy difference from Sb ions contributes 74% to the total strain energy difference. In addition, we find that the difference mainly comes from the deviation of the Al-Sb-Al bond angles from the ideal value (109.47°). In chalcopyrite $AlP_{0.5}Sb_{0.5}$ alloy, the maximum deviation of the Al-Sb-Al bond angles is 5.4°, much larger than that (2.7°) in WZ $AlP_{0.5}Sb_{0.5}$ alloy.

The DFT ground state energies of ZBAs with $x=0.25$ and 0.75 are chosen to be the lowest among the energies of the famatinite, Q8, and Q16 structures. Clearly, either Q8 or Q16 is found to be the DFT ground state structure for all considered ZBAs with $x=0.25$ and 0.75. These results are consistent with our previous study.[21] The calculated DFT formation enthalpy difference [$d\Delta H_f = \Delta H_f(WZA) - \Delta H_f(ZBA)$, where $\Delta H_f(WZA)$ [$\Delta H_f(ZBA)$] is the formation enthalpy of the WZA (ZBA) defined in Eq. (1)] are shown in Table III. We see that it follows the same trend as the strain energy difference, i.e., the GS WZA always has lower formation enthalpy than the corresponding ZBA. However, the lower formation enthalpy in the WZA does not necessarily mean that the WZA has lower total energy than the ZBA because the formation enthalpy are defined with respect to the pure bulk compounds with the *same* lattice structure, whereas the total-energy difference between the WZ and ZB $A_xB_{1-x}C$ alloys should also include the bond energy difference (dE_b) between the WZ and ZB phases of the parent binary compounds. We define $E_{WZ-ZB}(AC)$ [$E_{WZ-ZB}(BC)$] as the energy difference between the WZ and ZB phases of the AC (BC) compound. The bond energy difference $dE_b(x)$ between the WZA and ZBA as a function of x are then defined as:

$$dE_b(x) = xE_{WZ-ZB}(AC) + (1-x)E_{WZ-ZB}(BC). \quad (2)$$

The total-energy difference between the WZA and ZBA can then be calculated as

$$dE_{tot} = d\Delta H_f + dE_b. \quad (3)$$

It is clear from Eq. (3) that only when the formation enthalpy difference ($d\Delta H_f$) is more negative than $-dE_b$, the WZA can be more stable than the ZBA.

The DFT total-energy calculations are performed to determine which alloy structure is the GS phase of $Ga_xIn_{1-x}N$, AlP_xSb_{1-x}, ZnS_xTe_{1-x}, and GaP_xAs_{1-x} with $x=0.25$, 0.5, and 0.75. For the parent compounds, we find that the energy differences E_{WZ-ZB} between the WZ and ZB phases are −5.6, −10.8, 3.5, 6.5, 3.2, 6.0, 8.8, and 11.4 meV/atom for GaN, InN, AlP, AlSb, ZnS, ZnTe, GaP, and GaAs, respectively. In agreement with previous first-principles calculations[5] and experimental observations, we find that GaN and InN have the WZ GS structure, whereas the other compounds take the ZB phase as the most stable structure. The DFT results from the alloy calculations are summarized in Table III. For alloys with WZ binary constituents (InN and GaN) or small lattice-mismatched ZB binary constituents (GaP and GaAs), the GS alloy structure ($Ga_xIn_{1-x}N$ and GaP_xAs_{1-x}) is the same as the parent compounds. However, for $AlP_{0.5}Sb_{0.5}$, $AlP_{0.75}Sb_{0.25}$, $ZnS_{0.5}Te_{0.5}$, and $ZnS_{0.75}Te_{0.25}$, the WZA structure is the GS phase despite that the alloys are formed from ZB parent compounds. It is interesting to note that compounds such as MnTe (CdO), which has the stable NiAs (rocksalt) structure can be stabilized in the ZB phase by alloying it with ZB compounds.[33,34] Here we show that the alloy can be stabilized in a structure that is *different from both parent structures*. This remarkable alloy stabilized wurtzite structures originate from the fact that the gain in the strain energy relaxation when forming the WZA is larger than the average of the bond energy difference between the ZB and WZ phases. For example, $d\Delta H_f = -6.50$ meV/atom and $dE_b = 5.01$ meV/atom for $AlP_{0.5}Sb_{0.5}$. It is also interesting to see that, the alloy stabilization energy $d\Delta H_f$ for $A_{0.75}B_{0.25}C$ is larger than $A_{0.25}B_{0.75}C$, i.e., the WZA is more

favored when a large atom is mixed into a smaller host than a smaller atom is mixed into a large host.

In summary, we have identified the GS structures of the $A_xB_{1-x}C$ WZAs with $x=0.25$, 0.5, and 0.75. Using VFF and DFT calculations, we show that the GS WZA always has a lower strain energy and formation enthalpy than the corresponding ZBA, and thus the strain relaxation favors the formation of the WZA. We confirm this idea by showing that GS WZ AlP_xSb_{1-x} and ZnS_xTe_{1-x} with $x=0.25$, 0.5, and 0.75

are more stable than the corresponding ZBAs although their parent structures crystallize in the ZB phase.

[1] C.-Y. Yeh, S.-H. Wei, and A. Zunger, Phys. Rev. B **50**, 2715 (1994).

[2] M. van Schlfgaarde, A. Sher, and A.-B. Chen, J. Cryst. Growth **178**, 8 (1997).

[3] L. Sugiura, J. Appl. Phys. **81**, 1633 (1997).

[4] A. Garcia and M. L. Cohen, Phys. Rev. B **47**, 4215 (1993).

[5] Chin-Yu Yeh, Z. W. Lu, S. Froyen, and A. Zunger, Phys. Rev. B **45**, 12130 (1992); **46**, 10086 (1992).

[6] J. C. Phillips, *Bonds and Bands in Semiconductors* (Academic, New York, 1973).

[7] J. St. John and A. N. Bloch, Phys. Rev. Lett. **33**, 1095 (1974).

[8] J. R. Chelikowsky and J. C. Phillips, Phys. Rev. B **17**, 2453 (1978).

[9] G. Patriarche, F. Glas, M. Tchernycheva, C. Sartel, L. Largeau, and J.-C. Harmand, Nano Lett. **8**, 1638 (2008).

[10] M. Koguchi, H. Kakibayashi, M. Yazawa, K. Hiruma, and T. Katsuyama, Jpn. J. Appl. Phys. **31**, 2061 (1992).

[11] C. X. Shan, Z. Liu, X. T. Zhang, C. C. Wong, and S. K. Hark, Nanotechnology **17**, 5561 (2006).

[12] T. Akiyama, K. Sano, K. Nakamura, and T. Ito, Jpn. J. Appl. Phys. **45**, L275 (2006).

[13] V. G. Dubrovskii and N. V. Sibirev, Phys. Rev. B **77**, 035414 (2008).

[14] G. M. Dalpian and S.-H. Wei, Phys. Rev. Lett. **93**, 216401 (2004).

[15] G. M. Dalpian, Y. Yan, and S.-H. Wei, Appl. Phys. Lett. **89**, 011907 (2006).

[16] V. K. Lazarov, J. Zimmerman, S. H. Cheung, L. Li, M. Weinert, and M. Gajdardziska-Josifovska, Phys. Rev. Lett. **94**, 216101 (2005).

[17] S.-H. Wei, L. G. Ferreira, and A. Zunger, Phys. Rev. B **41**, 8240 (1990).

[18] L. G. Ferreira, S.-H. Wei, and A. Zunger, Phys. Rev. B **40**, 3197

[19] Z. W. Lu, D. B. Laks, S.-H. Wei, and A. Zunger, Phys. Rev. B **50**, 6642 (1994).

[20] J. Z. Liu, G. Trimarchi, and A. Zunger, Phys. Rev. Lett. **99**, 145501 (2007).

[21] S. Chen, X. G. Gong, and S.-H. Wei, Phys. Rev. B **77**, 073305 (2008).

[22] H. J. Xiang, S.-H. Wei, J. L. F. Da Silva, and J. Li, Phys. Rev. B **78**, 193301 (2008).

[23] P. Keating, Phys. Rev. **145**, 637 (1966).

[24] R. Martin, Phys. Rev. B **1**, 4005 (1970).

[25] J. L. Martins and A. Zunger, Phys. Rev. B **30**, 6217 (1984).

[26] K. Kim, W. R. L. Lambrecht, and B. Segall, Phys. Rev. B **53**, 16310 (1996).

[27] Our first-principles DFT calculations were performed on the basis of the projector-augmented wave method (Ref. 28) encoded in the Vienna *ab initio* simulation package (Ref. 29) using the local-density approximation (Ref. 30). For relaxed structures, the atomic forces are less than 0.01 eV/Å.

[28] P. E. Blöchl, Phys. Rev. B **50**, 17953 (1994); G. Kresse and D. Joubert, *ibid.* **59**, 1758 (1999).

[29] G. Kresse and J. Furthmüller, Comput. Mater. Sci. **6**, 15 (1996); Phys. Rev. B **54**, 11169 (1996).

[30] J. P. Perdew and A. Zunger, Phys. Rev. B **23**, 5048 (1981).

[31] R. Magri, S.-H. Wei, and A. Zunger, Phys. Rev. B **42**, 11388 (1990).

[32] For each bond involving the atom i, half of bond-stretching energy is contributed to the atom i. The bond-bending energy contributions from atom i include all bond angles which are centered at atom i.

[33] S.-H. Wei and A. Zunger, Phys. Rev. Lett. **56**, 2391 (1986).

[34] Y. Z. Zhu, G. D. Chen, H. Ye, A. Walsh, C. Y. Moon, and S.-H. Wei, Phys. Rev. B **77**, 245209 (2008).

(1989).